2018 26th Mediterranean Conference on Control and Automation (MED)
Zadar, Croatia, June 19-22, 2018

Adaptive Generalized Dynamic Inversion based Trajectory Tracking Control of Autonomous Underwater Vehicle

Uzair Ansari[1] Abdulrahman H. Bajodah[2] and Saqib Alam[3]

Abstract— **This paper presents the two-loops structured control system based on Adaptive Generalized Dynamic Inversion (AGDI) for the position and attitude control of Autonomous Underwater Vehicle (AUV). The outer-loop is responsible to provide the pitch and yaw tilting commands to the inner-loop, which in turns generates the tilting angles that are required to control its position in depth and east directions respectively. In AGDI control, the particular part is formulated by prescribing the constraint differential equations based on the deviation functions of the position coordinates and attitude angles. The control law is realized by inverting the constraint dynamics using Moore-Penrose Generalized Inverse (MPGI). The involved null control vector in the auxiliary part of AGDI is constructed to guarantee global closed loop stability of the linear and angular velocities. The singularity problem is addressed by incorporating a dynamic scaling factor in the expression of MPGI. The integration of an additional term based on Sliding Mode Control with adaptive modulation gain provides robustness against system nonlinearities, uncertainties and tracking performance deterioration due to dynamic scaling, such that semi-global practically stable position and attitude tracking is guaranteed. To demonstrate the tracking performance of the AGDI control, numerical simulations are conducted on six degrees of freedom simulator of the Monterey Bay Aquarium Research Institute (MBARI) AUV, under nominal and perturbed marine conditions.**

I. INTRODUCTION

Autonomous Underwater Vehicles (AUVs) are gaining more interest in scientific research communities because of the large benefits that they provide to mankind in both commercial and in military applications, see [1].

Among the factors that make it challenging to design an AUV control system are the highly nonlinear and coupled dynamics, in addition to uncertainties in hydrodynamic parameters, external disturbances, and un-modeled vehicle's dynamics. The AUV control methodologies that have been proposed in the literature include linear control, see [2], Sliding Mode Control (SMC), see [3], Fuzzy and Neural network control, see [4], [5].

One simple nonlinear control design approach is Nonlinear Dynamic Inversion (NDI), in which the control law is formulated to eliminate system nonlinearities by means of the feedback, see [6]. The NDI control technique in turns allows to incorporate well established linear control techniques. Regardless of these attributes, NDI has several shortcomings and limitations, including useful nonlinearity cancellation, large control effort, and numerical singularity configurations of square matrix inversion.

A new inversion-based control design methodology is Generalized Dynamic Inversion (GDI), in which dynamic constraints are prescribed in the form of differential equations that encapsulate the control objectives, and are generalized inverted using the Moore-Penrose Generalized Inverse (MPGI) based on Greville method, see [7], to obtain the control law. The GDI control technique has been applied to numerous engineering problems, see [8], [9], [10], [11], [12], [13], [14], [15], [16].

The GDI control methodology allows for two cooperating controllers that act on two orthogonally complement control spaces: one is the particular controller that realizes the dynamic constraints, and the other is the auxiliary controller that is affine in the null control vector, and provides extra degree of control design freedom.

In this paper Adaptive Generalized Dynamic Inversion (AGDI) control is designed for the position and attitude tracking of AUV. In the outer (position) loop, AGDI is applied to generate the desired pitch and yaw attitude commands based on the depth and the east positional errors respectively. In the inner (attitude) loop, AGDI control is responsible to follow the pitch and yaw attitude angles towards their desired values. The singularity issue due to non-square inversion is avoided via augmenting a dynamic scaling factor with MPGI. To provide robustness, an additional term based on SMC with adaptive modulation gain is included with conventional GDI that makes it AGDI. This approach will guarantee semi-global practically stable position and attitude tracking. Numerical simulations are conducted on a six Degree of Freedom (DOFs) simulator of the Monterey Bay Aquarium Research Institute (MBARI) AUV, see [17], to analyze the performance of the AGDI control law.

This paper is organized as follows. Section. II briefly explain the mathematical modeling of MBARI AUV. The control structure and the formulation of GDI control for the inner and the outer loops are presented in Section III. The singularity issue and its rectification is discussed in Section. IV. The design of hybrid GDI-SMC control is presented in Section. V, whereas its practical stability analysis is provided in Section. VI. Finally, simulation results and conclusion are presented in Sections. VII and VIII respectively.

[1]Uzair Ansari is Research Scholar at Department of Aeronautical Engineering, King Abdulaziz University, P.O.Box 80204, Jeddah 21589, Saudi Arabia uzansari@hotmail.com

[2]Abdulrahman H. Bajodah is with the Faculty of Aeronautical Engineering, King Abdulaziz University, P.O.Box 80204, Jeddah 21589, Saudi Arabia abajodah@kau.edu.sa

[3]Saqib Alam is Research Scholar at Department of Mechanical Engineering, NED University, Karachi, Pakistan alam.saqib@gmail.com

II. Mathematical modeling

The data of the MBARI variable length AUV is shown in Table I, see [17]. The MBARI AUV contains the articulated ring-wing control surface with a ducted propeller. The rudder and elevator commands are executed by moving a double gimbal mechanism to actuate the ring-wing and thruster. The vehicle is inherently stable in roll axis, hence no roll control input is needed.

TABLE I
MBARI specifications

Parameters	values	units
Length, L	5.554	m
Diameter, d	0.533	m
Mass, m	1093.1	kg
Moment of inertia about x_B, J_x	36.677	$kg.m^2$
Moment of inertia about y_B, J_y	2154.3	$kg.m^2$
Moment of inertia about z_B, J_z	2154.3	$kg.m^2$
Thrust, T_p	52.0	N
Max. deflections of δ_θ and δ_ψ	± 15.0	deg

A. Coordinate system and reference frames

The two reference frames used in deriving the AUV six DOFs equations of motion are the North-East-Depth earth-fixed frame F_E and the body-fixed frame F_B. The attitude roll, pitch, and yaw angles are denoted by ϕ, θ, and ψ, respectively. The translational surge, sway, and heave velocities of the cg are denoted in F_B by u, v, and w, and the roll, pitch, and yaw angular velocities of F_B relative to F_E are denoted in F_B by p, q, and r, respectively.

B. Kinematical equations of motion

The kinematical equations of motion of AUV are given as

$$\begin{bmatrix} \dot{x}_e \\ \dot{y}_e \\ \dot{z}_e \\ \dot{\phi} \\ \dot{\theta} \\ \dot{\psi} \end{bmatrix} = \begin{bmatrix} \mathbf{T_1} & 0_{3x3} \\ 0_{3x3} & \mathbf{T_2} \end{bmatrix} \begin{bmatrix} u \\ v \\ w \\ p \\ q \\ r \end{bmatrix} \tag{1}$$

where $\mathbf{T_1}$ and $\mathbf{T_2}$ are the transformation matrices, see [4].

C. Dynamical equations of motion

The following are the six DOFs equations of motion for an AUV in F_B, [4], [17]

$$m[\dot{u} - vr + wq - x_g(q^2 + r^2) + y_g(pq - \dot{r}) + z_g(pr + \dot{q})] = \Sigma X_{ext} \tag{2}$$

$$m[\dot{v} - wp + ur - y_g(p^2 + r^2) + z_g(pr - \dot{q}) + x_g(qp - \dot{r})] = \Sigma Y_{ext} \tag{3}$$

$$m[\dot{w} - uq + vp - z_g(q^2 + p^2) + x_g(pr - \dot{q}) + y_g(rq - \dot{p})] = \Sigma Z_{ext} \tag{4}$$

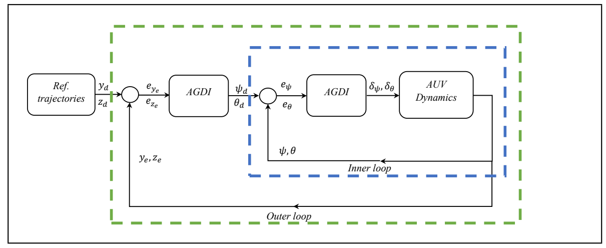

Fig. 1. Control architecture

$$J_x\dot{p} + (J_z - J_y)qr + m[y_g(\dot{w} - uq + vp) - z_g(\dot{v} - wp + ur)] = \Sigma K_{ext} \tag{5}$$

$$J_y\dot{q} + (J_x - J_z)rp + m[z_g(\dot{u} - vr + wq) - x_g(\dot{w} - uq + vp)] = \Sigma M_{ext} \tag{6}$$

$$J_z\dot{r} + (J_y - J_x)pq + m[x_g(\dot{v} - wp + ur) - y_g(\dot{u} - vr + wq)] = \Sigma N_{ext} \tag{7}$$

The comprehensive details of the external forces and moments in the right hand sides of (2 - 7) and the description of the force and moment coefficients are found in [17].

III. GDI control design

A two-loops structure of a slow (outer) positional loop and a fast (inner) attitude loop is constructed to control the under-actuated AUV dynamics, see Fig. 1. The outer-loop utilizes AGDI, to generate the desired pitch θ_d and yaw ψ_d commands based on the positional errors along z_e and y_e directions respectively. The inner-loop in turns uses AGDI to produce the control deflections δ_θ and δ_ψ required to track the desired pitch and yaw attitude commands. The state vector of AUV is decomposed into the inner attitude state vector $\mathbf{x_i} = [\theta \ \psi]^T$ and the outer position state vector $\mathbf{x_o} = [y_e \ z_e]^T$.

A. GDI control for inner attitude loop

The differential equations of the body Euler's angles θ and ψ are written in compact form as

$$\dot{\mathbf{x}}_i = \mathbf{H}(\mathbf{x}_i)\mathbf{x}_r \tag{8}$$

where $\mathbf{H}(\mathbf{x}_i)$ is given as

$$\mathbf{H}(\mathbf{x}_i) = \begin{bmatrix} cos\phi & -sin\phi \\ sin\phi/cos\theta & cos\phi/cos\theta \end{bmatrix} \tag{9}$$

and $\mathbf{x}_r = [q \ \ r]^T$ is the angular velocity vector. The differential equations of the angular velocity dynamics $\dot{\mathbf{x}}_r$ are given as

$$\dot{\mathbf{x}}_r = \mathbf{A}_r(\mathbf{x}_i, \mathbf{x}_r) + \mathbf{B}_r\mathbf{u}_i \tag{10}$$

where

$$\mathbf{A}_r = \begin{bmatrix} [-(J_x - J_z)rp - m\{z_g(\dot{u} - vr + wq) - x_g(\dot{w} \\ -uq + vp)\} + M_{\dot{w}}\dot{w} + M_{rp}rp + M_q uq + M_w uw \\ +M_{w|w|}w|w| + M_{q|q|}q|q| - (x_g W - x_b B) \\ \cos\theta\cos\phi - (z_g W - z_b B)\sin\theta]/(J_y - M_{\dot{q}}) \\ \\ [-(J_y - J_x)pq + m\{x_g(\dot{v} - wp + ur) - y_g(\dot{u} \\ -vr + wq)\} + N_{\dot{v}}\dot{v} + N_{pq}pq + N_r ur + N_v uv \\ +N_{r|r|}r|r| + N_{v|v|}v|v| - (x_g W - x_b B) \\ \cos\theta\sin\phi + (y_g W - y_b B)\sin\theta]/(J_z - N_{\dot{r}}) \end{bmatrix},$$

$$\mathbf{B}_r = \begin{bmatrix} -T_p x_R/(J_y - M_{\dot{q}}) & 0 \\ 0 & T_p x_R/(J_z - N_{\dot{r}}) \end{bmatrix}, \mathbf{u}_i = \begin{bmatrix} \delta_\theta \\ \delta_\psi \end{bmatrix}$$

1) Formulation of constraint dynamics: To construct the constraint differential equation, the weighted error norm of the attitude deviation function is defined as

$$\xi_i = a_1 e_\theta^2 + a_2 e_\psi^2 = \mathbf{e}_i^T \mathbf{D}(a_1, a_2)\mathbf{e}_i \tag{11}$$

where $\mathbf{e}_i = [e_\theta \; e_\psi]^T$, a_1, a_2 are the positive real valued constants and $\mathbf{D}(a_1, a_2)$ denotes the diagonal matrix. Based on the deviation function, a linear time-varying ordinary differential constraint equation is formulated, whose order is proportional to the relative degree of the deviation function. The equation takes the form

$$\ddot{\xi}_i + c_1(t)\dot{\xi}_i + c_2(t)\xi_i = 0 \tag{12}$$

where c_1 and c_2 are chosen such that the constraint dynamic is uniformly asymptotically stable [18]. The first and the second time derivatives of constraint dynamics are computed as

$$\dot{\xi}_i = 2\mathbf{e}_i^T \mathbf{D}(a_1, a_2)(\mathbf{H}\mathbf{x}_r - \dot{\mathbf{x}}_{id}) \tag{13}$$

$$\ddot{\xi}_i = 2\mathbf{e}_i^T \mathbf{D}(a_1, a_2)\{\mathbf{H}(\mathbf{A}_r + \mathbf{B}_r\mathbf{u}_i) + \dot{\mathbf{H}}\mathbf{x}_r - \ddot{\mathbf{x}}_{id}\} \tag{14}$$

By placing the time derivatives, the algebraic form of the constraint differential equation given by (12) is written as

$$\mathcal{A}_i(\mathbf{x}_i, t)\mathbf{u}_i = B_i(\mathbf{x}_i, \mathbf{x}_r, t) \tag{15}$$

where

$$\mathcal{A}_i = [2\mathbf{e}_i^T \mathbf{D}(a_1, a_2)\mathbf{H}(\mathbf{x}_i)\mathbf{B}_r], \tag{16}$$

$$\begin{aligned} B_i = -2\mathbf{e}_i^T \mathbf{D}(a_1, a_2)(-\ddot{\mathbf{x}}_{id} + \dot{\mathbf{H}}(\mathbf{x}_i)\mathbf{H}(\mathbf{x}_i)^{-1}\mathbf{x}_{id} \\ + \mathbf{H}(\mathbf{x}_i)\mathbf{A}_r(\mathbf{x}_i, \mathbf{x}_r) - 2\dot{\mathbf{e}}_i^T \mathbf{D}(a_1, a_2)\dot{\mathbf{e}}_i \\ - 2c_1\mathbf{e}_i^T \mathbf{D}(a_1, a_2)\dot{\mathbf{e}}_i - c_2[a_1, a_2]\dot{\mathbf{e}}_i \end{aligned} \tag{17}$$

Equation (15) is an under-determined algebraic system that has infinite number of solutions. The general solution of this system is given by the Greville method, resulting in

$$\mathbf{u}_i = \mathcal{A}_i^+(\mathbf{x}_i, t)B_i(\mathbf{x}_i, \mathbf{x}_r, t) + \mathbf{P}_i(\mathbf{x}_i, t)\boldsymbol{\lambda}_i \tag{18}$$

where $\boldsymbol{\lambda}_i \in R^2$ is null control vector, $\mathcal{A}_i^+$ is the MPGI of $\mathcal{A}_i$, given by,

$$\mathcal{A}_i^+(\mathbf{x}_i, t) = \mathcal{A}_i^T(\mathbf{x}_i, t)\left\{\mathcal{A}_i(\mathbf{x}_i, t)\mathcal{A}_i^T(\mathbf{x}_i, t)\right\}^{-1} \tag{19}$$

and $\mathbf{P}_i$ is the null projection matrix given by

$$\mathbf{P}_i(\mathbf{x}_i, t) = \mathbf{I}_{2\times 2} - \mathcal{A}_i^+(\mathbf{x}_i, t)\mathcal{A}_i(\mathbf{x}_i, t) \tag{20}$$

where $\mathbf{I}_{2\times 2}$ is the 2×2 identity matrix. By placing the control expression given by (18) in (10), $\dot{\mathbf{x}}_r$ is written as

$$\begin{aligned} \dot{\mathbf{x}}_r = \mathbf{A}_r(\mathbf{x}_i, \mathbf{x}_r, t) + \mathbf{B}_r\{\mathcal{A}_i^+(\mathbf{x}_i, t)B_i(\mathbf{x}_i, \mathbf{x}_r, t) \\ + \mathbf{P}_i(\mathbf{x}_i, t)\boldsymbol{\lambda}_i\} \end{aligned} \tag{21}$$

B. Null control vector design for angular rate stabilization

The null control vector $\boldsymbol{\lambda}_i$ is contructed with the aid of a control Lyapunov function to stabilize the angular velocities, resulting in

$$\mathbf{P}_i\boldsymbol{\lambda}_i = -(\bar{\mathbf{P}}_i\mathbf{B}_r)^{-1}\left(\bar{\mathbf{P}}_i\boldsymbol{\Delta}_i + \frac{\dot{\mathbf{P}}_i\mathbf{e}_r}{2} + \frac{\mathbf{Q}_i\mathbf{e}_r}{2}\right) \tag{22}$$

where $\mathbf{e}_r = [p - p_d(t) \; q - q_d(t)]^T$. By placing the expression of $\mathbf{P}_i\boldsymbol{\lambda}_i$ in (18), the control law takes the following form

$$\mathbf{u}_i = \mathcal{A}_i^+ B_i - (\bar{\mathbf{P}}_i\mathbf{B}_r)^{-1}\left(\bar{\mathbf{P}}_i\boldsymbol{\Delta}_i + \frac{\dot{\mathbf{P}}_i\mathbf{e}_r}{2} + \frac{\mathbf{Q}_i\mathbf{e}_r}{2}\right) \tag{23}$$

Theorem 1: The control law given by (23) guarantees global closed-loop stability of the angular velocity dynamics $\dot{\mathbf{x}}_r$.

Proof: Let the null control vector $\boldsymbol{\lambda}_i$ is designed to be a linear function of the angular velocity error vector, defined as

$$\boldsymbol{\lambda}_i = \mathbf{K}_i\mathbf{e}_r \tag{24}$$

where $\mathbf{K}_i$ is the 2×2 gain matrix. By placing $\boldsymbol{\lambda}_i$ in (21), angular velocity dynamics $\dot{\mathbf{x}}_r$ becomes

$$\begin{aligned} \dot{\mathbf{x}}_r = \mathbf{A}_r(\mathbf{x}_i, \mathbf{x}_r, t) + \mathbf{B}_r\{\mathcal{A}_i^+(\mathbf{x}_i, t)B_i(\mathbf{x}_i, \mathbf{x}_r, t) \\ + \mathbf{P}_i\mathbf{K}_i\mathbf{e}_r\} \end{aligned} \tag{25}$$

The desired body angular velocities are defined as

$$\dot{\mathbf{x}}_{rd} = \mathbf{A}_r(\mathbf{x}_i, \mathbf{x}_{rd}, t) + \mathbf{B}_r\{\mathcal{A}_i^+(\mathbf{x}_i, t)B_i(\mathbf{x}_i, \mathbf{x}_{rd}, t)\} \tag{26}$$

The error dynamics acquired by subtracting (26) from (25), and after some simplification yields

$$\dot{\mathbf{e}}_r = \boldsymbol{\Delta}_i(\mathbf{x}_i, \mathbf{x}_r, \mathbf{x}_{rd}, t) + \mathbf{B}_r\mathbf{P}_i(\mathbf{x}_i, t)\mathbf{K}_i\mathbf{e}_r \tag{27}$$

where,

$$\begin{aligned} \boldsymbol{\Delta}_i = \mathbf{A}_r(\mathbf{x}_i, \mathbf{x}_r, t) - \mathbf{A}_r(\mathbf{x}_i, \mathbf{x}_{rd}, t) + \mathbf{B}_r\mathcal{A}_i^+(\mathbf{x}_i, t) \\ \{B_i(\mathbf{x}_i, \mathbf{x}_r, t) - B_i(\mathbf{x}_i, \mathbf{x}_{rd}, t)\} \end{aligned} \tag{28}$$

Now consider the control Lyapunov function

$$V_{\lambda_i}(\mathbf{e}_r, \mathbf{x}_i, \mathbf{x}_r, t) = \mathbf{e}_r{}^T\bar{\mathbf{P}}_i(\mathbf{x}_i, t)\mathbf{e}_r \tag{29}$$

where $\bar{\mathbf{P}}_i(\mathbf{x}_i, t) = \mathbf{P}_i + \varepsilon\mathbf{I}_{2\times 2}$ for an arbitrary positive scalar ε. The time derivative of V_{λ_i} along the AUV trajectories is

$$\dot{V}_{\lambda_i} = \mathbf{e}_r{}^T(2\bar{\mathbf{P}}_i\boldsymbol{\Delta}_i + 2\bar{\mathbf{P}}_i\mathbf{B}_r\mathbf{P}_i\mathbf{K}_i\mathbf{e}_r + \dot{\mathbf{P}}_i\mathbf{e}_r) \tag{30}$$

A sufficient condition for the global asymptotic stability is that $\dot{V}_{\lambda_i} < 0$ along the AUV state trajectories. This can be assured by the existence of a symmetric positive definite matrix $\mathbf{Q}_i$ such that

$$\dot{V}_{\lambda_i} = -\mathbf{e}_r{}^T\mathbf{Q}_i\mathbf{e}_r < 0 \tag{31}$$

Hence, equating (30) and (31) yields

$$2\bar{\mathbf{P}}_i\boldsymbol{\Delta}_i + 2\bar{\mathbf{P}}_i\mathbf{B}_r\mathbf{P}_i\mathbf{K}_i\mathbf{e}_r + \dot{\mathbf{P}}_i\mathbf{e}_r + \mathbf{Q}_i\mathbf{e}_r = \mathbf{0}_2 \quad (32)$$

Solving for the projected gain $\mathbf{P}_i\mathbf{K}_i\mathbf{e}_r$ or $\mathbf{P}_i\boldsymbol{\lambda}_i$ yields

$$\mathbf{P}_i\boldsymbol{\lambda}_i = -\left(\bar{\mathbf{P}}_i\mathbf{B}_r\right)^{-1}\left(\bar{\mathbf{P}}_i\boldsymbol{\Delta}_i + \frac{\dot{\mathbf{P}}_i\mathbf{e}_r}{2} + \frac{\mathbf{Q}_i\mathbf{e}_r}{2}\right) \quad (33)$$

The null control vector given by (33), provides global asymptotic stability to the angular velocity dynamics. ■

C. GDI control for outer position loop

To generate the desired pitch θ_d and yaw ψ_d commands, the nonlinear dynamics of $\dot{y}_e$ and $\dot{z}_e$ as shown by second and third rows of (1) is linearized about the instantaneous values of θ and ψ, by using the small disturbance theory [19], which implies

$$\begin{aligned}\dot{y}_{ed} &= (c_{\psi+\Delta\psi_d}c_{\theta+\Delta\theta_d})u + (c_\phi s_{\theta+\Delta\theta_d}s_{\psi+\Delta\psi_d} \\ &- c_\phi s_{\psi+\Delta\psi_d})v + (s_{\psi+\Delta\psi_d}s_\phi - c_\phi s_{\theta+\Delta\theta_d}c_{\psi+\Delta\psi_d})w \quad (34)\end{aligned}$$

$$\dot{z}_{ed} = -s_{\theta+\Delta\theta_d}u + c_{\theta+\Delta\theta_d}s_\phi v + c_\phi c_{\theta+\Delta\theta_d}w \quad (35)$$

The two command angles are set to be $\theta_d = \theta + \Delta\theta_d$ and $\psi_d = \psi + \Delta\psi_d$. Expanding the trigonometric functions, yields the following linear approximate expressions

$$\begin{bmatrix}\dot{y}_{ed}\\ \dot{z}_{ed}\end{bmatrix} = \mathbf{M}_{2\times2}\begin{bmatrix}\Delta\theta_d\\ \Delta\psi_d\end{bmatrix} + \mathbf{N}_{2\times1} \quad (36)$$

where

$$\begin{aligned}
\mathbf{M}_{(1,1)} &= -us_\theta s_\psi + vs_\phi c_\theta s_\psi + wc_\phi c_\theta s_\psi\\
\mathbf{M}_{(1,2)} &= -uc_\theta - vs_\theta s_\phi - ws_\theta c_\phi\\
\mathbf{M}_{(2,1)} &= uc_\theta c_\psi + v(s_\phi s_\theta c_\psi - c_\phi s_\psi) + w(s_\phi s_\psi - c_\phi s_\theta c_\psi)\\
\mathbf{M}_{(2,2)} &= 0\\
\mathbf{N}_{(1,1)} &= uc_\theta s_\psi + v(s_\phi s_\theta s_\psi + c_\phi c_\psi) + w(s_\theta c_\phi s_\psi - s_\phi c_\psi)\\
\mathbf{M}_{(2,1)} &= -us_\theta + vs_\phi c_\theta + wc_\phi c_\theta
\end{aligned}$$

1) Constraint dynamics formulation: The weighted error norm of the positional deviation functions is defined as

$$\xi_o = a_3 e_{y_e}^2 + a_4 e_{z_e}^2 = \mathbf{e}_o^T\mathbf{D}(a_3, a_4)\mathbf{e}_o \quad (37)$$

where a_3 and a_4 are positive real constants, and $\mathbf{e}_o = [e_{y_e}\ e_{z_e}]^T$ represents the positional error vector. The first and second time derivatives of ξ_o are

$$\dot{\xi}_o = 2\mathbf{e}_o^T\mathbf{D}(a_3, a_4)\dot{\mathbf{e}}_o \quad (38)$$

$$\ddot{\xi}_o = 2\dot{\mathbf{e}}_o^T\mathbf{D}(a_3, a_4)\dot{\mathbf{e}}_o + 2\mathbf{e}_o^T\mathbf{D}(a_3, a_4)\ddot{e}_o \quad (39)$$

Since the relative degree is 2, a second-order linear time-varying constraint dynamics is formulated as

$$\ddot{\xi}_o + c_3(t)\dot{\xi}_o + c_4(t)\xi_o = 0 \quad (40)$$

where the coefficients $c_3(t)$ and $c_4(t)$ are chosen such that the constraint dynamics given by (40) is uniformly asymptotically stable [18]. Substituting the time derivatives given by (38) and (39) into (40), the differential form of constraint dynamics transformed into the following under-determined algebraic form

$$\mathbf{A}_o(\mathbf{x}_o, t)\mathbf{u}_o = B_o(\mathbf{x}_o, t) \quad (41)$$

where

$$\mathbf{A}_o(\mathbf{x}_o, t) = 2\mathbf{e}_o^T\mathbf{D}(a_3, a_4)\mathbf{M}, \quad (42)$$

$$\begin{aligned}B_o(\mathbf{x}_o, t) &= 2\mathbf{e}_o^T\mathbf{D}(a_1, a_2)\left[\ddot{\mathbf{x}}_o - \mathbf{N}\right] + 2\dot{\mathbf{e}}_o^T\mathbf{D}(a_1, a_2)\dot{\mathbf{e}}_o\\ &+ 2c_1\mathbf{e}_o^T\mathbf{D}(a_1, a_2)\dot{\mathbf{e}}_o + c_2\mathbf{e}_o^T\mathbf{D}(a_1, a_2)\mathbf{e}_o \quad (43)\end{aligned}$$

and

$$\mathbf{u}_o = [\Delta\theta\ \ \Delta\psi]^T \quad (44)$$

The general solution of (41) is given by the Greville method resulting in

$$\mathbf{u}_o = \mathbf{A}_o^+(\mathbf{x}_o, t)B_o(\mathbf{x}_o, t) + \mathbf{P}_o(\mathbf{x}_o, t)\boldsymbol{\lambda}_o \quad (45)$$

where $\boldsymbol{\lambda}_o \in R^2$ is the null control vector and $\mathbf{P}_o$ is the null projection matrix.

2) Design of null control vector: The null control vector $\boldsymbol{\lambda}_o$ is designed by employing Lyapunov approach, to guarantee global closed-loop stability of the linear velocity dynamics $\dot{\mathbf{x}}_o = [\dot{y}_e\ \ \dot{z}_e]^T$, which is expressed by

$$\mathbf{P}_o\boldsymbol{\lambda}_o = \{\mathbf{M}\}^{-1}\left(2\mathbf{R}_o\ddot{\mathbf{e}}_o + \mathbf{Q}_o\boldsymbol{\Delta}_o\right) \quad (46)$$

By placing $\mathbf{P}_o\boldsymbol{\lambda}_o$ in (45), the control law becomes

$$\mathbf{u}_o = \mathbf{A}_o^+B_o + \{\mathbf{M}\}^{-1}\left(2\mathbf{R}_o\ddot{\mathbf{e}}_o + \mathbf{Q}_o\boldsymbol{\Delta}_o\right) \quad (47)$$

Theorem 2: The control law given by (47) guarantees global closed-loop stability of the linear velocity dynamics $\dot{\mathbf{x}}_o$.

Proof: Let the null control vector $\boldsymbol{\lambda}_o$ is designed to be a linear function of velocity error vector, defined as

$$\boldsymbol{\lambda}_o = \mathbf{K}_o\dot{\mathbf{e}}_o = \mathbf{K}_o(\dot{\mathbf{x}}_o - \dot{\mathbf{x}}_{od}) \quad (48)$$

where $\mathbf{K}_o$ represents the 2×2 gain matrix, and $\dot{\mathbf{x}}_{od} = [\dot{y}_{ed}\ \ \dot{z}_{ed}]^T$. The error dynamics $\dot{\mathbf{e}}_o$ is computed by subtracting $\dot{\mathbf{x}}_{od}$ from $\dot{\mathbf{x}}_o$, and after some simplification it yields

$$\dot{\mathbf{e}}_o = \boldsymbol{\Delta}_o - \mathbf{M}\mathbf{P}_o\mathbf{K}_o\dot{\mathbf{e}}_o \quad (49)$$

where $\boldsymbol{\Delta}_o = \dot{\mathbf{x}}_o - \mathbf{M}\mathcal{A}_o^+(\mathbf{x}_o, t)B_o(\mathbf{x}_o, t) - \mathbf{N}$. Now consider the control Lyapunov function

$$V_{\lambda_o}(\mathbf{x}_o, t) = \dot{\mathbf{e}}_o^T\mathbf{R}_o\dot{\mathbf{e}}_o \quad (50)$$

where the matrix $\mathbf{R}_o$ is a symmetric positive definite. The time derivative of the Lyapunov function is evolved as

$$\dot{V}_{\lambda_o} = 2\dot{\mathbf{e}}_o^T\mathbf{R}_o\ddot{\mathbf{e}}_o \quad (51)$$

For global asymptotic stability, we know that $\dot{V}_{\lambda_o} < 0\ \forall\ \dot{\mathbf{e}}_o \neq 0$. This can be assured by the presence of symmetric positive definite matrix $\mathbf{Q}_o$ such that

$$\dot{V}_{\lambda_o} = -\dot{\mathbf{e}}_o^T\mathbf{Q}_o\dot{\mathbf{e}}_o < 0 \quad (52)$$

Equating (51) with (52) yields

$$2\mathbf{R}_o\ddot{\mathbf{e}}_o + \mathbf{Q}_o(\boldsymbol{\Delta}_o - \mathbf{M}\mathbf{P}_o\mathbf{K}_o\dot{\mathbf{e}}_o) = 0 \quad (53)$$

The value of the projected gain $\mathbf{P}_o\mathbf{K}_o\dot{\mathbf{e}}_o$ is solved for from (53) as

$$\mathbf{P}_o\boldsymbol{\lambda}_o = \mathbf{P}_o\mathbf{K}_o\dot{\mathbf{e}}_o = \{\mathbf{M}\}^{-1}\left(2\mathbf{R}_o\ddot{\mathbf{e}}_o + \mathbf{Q}_o\boldsymbol{\Delta}_o\right) \quad (54)$$

The derived null control vector $\mathbf{P}_o\boldsymbol{\lambda}_o$ given by (54) guarantees global closed-loop asymptotic stability of the linear velocity dynamics. ■

IV. GDI SINGULARITY AVOIDANCE

Generalized inversion has its limitation when it is applied to matrices with variable elements, in what is referred to as generalized inversion singularity. This phenomenon is avoided in the present approach by appealing to Dynamically Scaled Generalized Inverse (DSGI) introduced in [18]. A first order dynamic scaling factor ν_i is introduced for the inner-loop dynamics, governed by

$$\dot{\nu}_i(t) = -\nu_i(t) + \frac{\gamma_i}{\|\mathbf{e}_i(t)\|^2},\ \nu_i(0) > 0 \quad (55)$$

where γ_i is a positive real valued constant and $\|\ .\ \|$ denotes the Euclidean norm. Now DSGI of $\mathcal{A}_i(\mathbf{x}_i, t)$ is written as

$$\mathcal{A}_i^*(\mathbf{x}_i, \nu_i, t) = \frac{\mathcal{A}_i^T(\mathbf{x}_i, t)}{\mathcal{A}_i(\mathbf{x}_i, t)\mathcal{A}_i^T(\mathbf{x}_i, t) + \nu_i(t)} \quad (56)$$

and control law given by (23) becomes

$$\mathbf{u}_i^* = \mathcal{A}_i^* B_i - (\bar{\mathbf{P}}_i\mathbf{B}_r)^{-1}\left(\bar{\mathbf{P}}_i\boldsymbol{\Delta}_i + \frac{\dot{\mathbf{P}}_i\mathbf{e}_r}{2} + \frac{\mathbf{Q}_i\mathbf{e}_r}{2}\right) \quad (57)$$

Similarly for the outer-loop dynamics, the DSGI of $\mathbf{A}_o(\mathbf{x}_o, t)$ is expressed as

$$\mathbf{A}_o^*(\mathbf{x}_o, \nu_o, t) = \frac{\mathbf{A}_o^T(\mathbf{x}_o, t)}{\mathbf{A}_o(\mathbf{x}_o, t)\mathbf{A}_o^T(\mathbf{x}_o, t) + \nu_o(t)} \quad (58)$$

where the dynamic scaling factor ν_o is defined as

$$\dot{\nu}_o(t) = -\nu_o(t) + \frac{\gamma_o}{\|\mathbf{e}_o(t)\|^2},\ \nu_o(0) > 0 \quad (59)$$

where γ_o is a positive real valued constant. Based on this, the modified form of GDI control law given by (47) becomes

$$\mathbf{u}_o^* = \mathbf{A}_o^* B_o + \{\mathbf{M}\}^{-1}\left(2\mathbf{R}_o\ddot{\mathbf{e}}_o + \mathbf{Q}_o\boldsymbol{\Delta}_o\right) \quad (60)$$

The detailed proof of the boundedness of DSGI is found in [10].

V. DESIGN OF AGDI CONTROLLER

This section presents the augmentation of SMC term having adaptive gain with GDI to make it AGDI, to enhance the robustness attributes. Let the hybrid SMC-GDI control law for the inner-loop attitude dynamics is constructed to be of the following form

$$\mathbf{u}_i^* = \mathcal{A}_i^* B_i + \mathbf{P}_i\boldsymbol{\lambda}_i - C_i\mathcal{A}_i^*\frac{s_i}{\|s_i\|} \quad (61)$$

where, C_i is the adaptive modulation gain defined as

$$C_i = \|\mathbf{u_i}_{eq}^*\|^T\hat{\mathbf{C}}_i + \eta_i \quad (62)$$

where $\|\mathbf{u_i}_{eq}^*\|$ represents the nominal GDI control given by (57) and η_i is the bound of uncertainties/disturbances which ensures the reaching condition. The adaptive gain $\hat{\mathbf{C}}_i$ evolves according to

$$\dot{\hat{\mathbf{C}}}_i = -k_1\hat{\mathbf{C}}_i + k_2\varepsilon_i\|\mathbf{u_i}_{eq}^*\|\|s_i\| \quad (63)$$

where k_1, k_2 and ε_i are the constant positive scalar gains, and s_i is the sliding surface variable defined as

$$s_i = \dot{\xi}_i + c_1(t)\xi_i + c_2(t)\int \xi_i dt \quad (64)$$

The time derivative of the sliding surfaces s_i is evaluated as

$$\dot{s}_i = \ddot{\xi}_i + c_1(t)\dot{\xi}_i + c_2(t)\xi_i \quad (65)$$

Notice that driving $\dot{s}_i$ to zero implies asymptotic realization of the constraint dynamic given by (12). Hence, let $\dot{s}_i$ is defined as

$$\dot{s}_i = \mathcal{A}_i(\mathbf{x}_i, t)\mathbf{u}_i^* - B_i(\mathbf{x}_i, \mathbf{x}_r, t) \quad (66)$$

Similarly hybrid SMC-GDI control law for outer-loop positional dynamics takes the following form

$$\mathbf{u}_o^* = \quad \mathbf{A}_o^* B_o + \mathbf{P}_o\boldsymbol{\lambda}_o - C_o\mathbf{A}_o^*\frac{s_o}{\|s_o\|} \quad (67)$$

where, C_o denotes the adaptive modulation gain, defined as

$$C_o = \|\mathbf{u_o}_{eq}^*\|^T\hat{\mathbf{C}}_o + \eta_o \quad (68)$$

where $\|\mathbf{u_o}_{eq}^*\|$ is the nominal GDI controller given by (60) and η_o is the bound of uncertainties and disturbances. The positive adaptation gain $\hat{\mathbf{C}}_o$ evolves according to

$$\dot{\hat{\mathbf{C}}}_o = -k_3\hat{\mathbf{C}}_o + k_4\varepsilon_o\|\mathbf{u_o}_{eq}^*\|\|s_o\| \quad (69)$$

where k_3, k_4, ε_o are the constant positive scalar gains and s_o is the sliding surface defined as

$$s_o = \dot{\xi}_o + c_3(t)\xi_o + c_4(t)\int \xi_o dt \quad (70)$$

and its time derivative is given by

$$\dot{s}_o = \mathbf{A}_o(\mathbf{x}_o, t)\mathbf{u}_o^* - B_o(\mathbf{x}_o, t) \quad (71)$$

VI. STABILITY ANALYSIS OF AGDI CONTROL

For stability analysis of the inner subsystem dynamics, substitute the expression of $\mathbf{u}_i^*$ given by (61) in (66) yields

$$\dot{s}_i = \mathcal{A}_i\left\{\mathcal{A}_i^* B_i + \mathbf{P}_i\boldsymbol{\lambda}_i - C_i\mathcal{A}_i^*\frac{s_i}{\|s_i\|}\right\} - B_i \quad (72)$$

Furthermore, substituting $\mathbf{P}_i$ given by (20) in (72) and using the relation $\mathcal{A}_i(\mathbf{x}_i, t)\mathcal{A}_i^+(\mathbf{x}_i, t) = 1$, the expression of $\dot{s}_i$ given by (72) reduces to

$$\dot{s}_i = \{\delta_i(\mathbf{x}_i, \nu_i, t) - 1)\}B_i - C_i\delta_i(\mathbf{x}_i, \nu_i, t)\frac{s_i}{\|s_i\|} \quad (73)$$

where $\delta_i(\mathbf{x}_i, \nu_i, t) = \mathcal{A}_i(\mathbf{x}_i, t)\mathcal{A}_i^*(\mathbf{x}_i, \nu_i, t)$. On the other hand, $\mathcal{A}_i(\mathbf{x}_i, t)\mathcal{A}_i^+(\mathbf{x}_i, t) = 1$ does not hold true for $\delta_i(\mathbf{x}_i, \nu_i, t)$. Nevertheless, because $\nu_i \in (0, \infty)$, it follows from (56) that

$$0 < \delta_i(\mathbf{x}_i, \nu_i, t) < 1 \quad (74)$$

for all $\mathcal{A}_i(\mathbf{x}_i, t) \neq \mathbf{0}_{1\times 2}$, and that

$$\lim_{t\to\infty} \delta_i(\mathbf{x}_i, \nu_i, t) = 0 \;\Leftrightarrow\; \lim_{t\to\infty} \mathcal{A}_i(\mathbf{x}_i, t) = \mathbf{0}_{1\times 2} \tag{75}$$

Consider a positive definite Lyapunov function as

$$V_i = \frac{1}{2} s_i^2 \tag{76}$$

The time derivative of V_i is evaluated as

$$\dot{V}_i = s_i \left\{ \delta_i(\mathbf{x}_i, \nu_i, t) - 1 \right\} B_i - C_i s_i \delta_i(\mathbf{x}_i, \nu_i, t) \frac{s_i}{\|s_i\|} \tag{77}$$

Therefore, a function C_i that satisfies

$$C_i(\mathbf{x}_i, \mathbf{x}_r, \nu_i, t) = \|\mathbf{u_i}^*_{eq}\|^T \hat{\mathbf{C}}_i + \eta_i > \frac{\delta_i - 1}{\delta_i} |B_i| \tag{78}$$

would guarantee $\dot{V}_i$ to be negative definite, and hence finite time stability of $s_i = 0$ follows from Lyapunov's direct method, [20]. Similarly to prove stability for the outer position loop, a function C_o that satisfies

$$C_o(\mathbf{x}_o, \nu_o, t) = \|\mathbf{u_o}^*_{eq}\|^T \hat{\mathbf{C}}_o + \eta_o > \frac{\delta_o - 1}{\delta_o} |B_o| \tag{79}$$

would guarantees $\dot{V}_o$ to be negative definite, and hence guarantees finite time convergence of $s_o = 0$.

However to guarantee negative definiteness of $\dot{V}_i$ and $\dot{V}_o$ and finite time convergence of s_i and s_o to zero, requires the function $C_i(\mathbf{x}_i, \mathbf{x}_r, \nu_i, t)$ and $C_o(\mathbf{x}_o, \nu_o, t)$ to reach infinite values or in other words, it needs η_i and η_o to reach infinite values as e_i and e_o vanishes respectively, which yields

$$\lim_{\mathbf{e}_i \to \mathbf{0}_{2\times 1}} \frac{\delta_i - 1}{\delta_i} = \lim_{\mathbf{e}_o \to \mathbf{0}_{2\times 1}} \frac{\delta_o - 1}{\delta_o} = -\infty$$

Therefore it is not feasible to design a SMC gains that guarantees finite time closed loop stability of the AGDI sliding mode dynamics, however it can be designed to achieve semi-global practical stability. In this section, semi-global practical stability is proved for inner subsystem attitude dynamics. The same methodology has being adopted to prove semi-global practical stability for outer subsystem positional dynamics.

Theorem 3: For every real number $\delta_i^* \in (0, 1)$ there exists a real number $\eta_i^* > 0$ such that the time derivative of V_i along solution trajectories of the sliding mode dynamics given by (73) is strictly negative for all $\delta_i(\mathbf{x}_i, \nu_i, t) > \delta_i^*$ and $\eta_i > \eta_i^*$.

Proof: Let δ_i^* be a prescribed constant real scalar in the range of $\delta_i(\mathbf{x}_i, \nu_i, t)$, i.e., $\delta_i^* \in (0, 1)$. Also, define $\bar{\eta}_i(\mathbf{x}_i, \mathbf{x}_r, t)$ as

$$\bar{\eta}_i(\mathbf{x}_i, \mathbf{x}_r, t) = -\frac{\delta_i^* - 1}{\delta_i^*} |B_i(\mathbf{x}_i, \mathbf{x}_r, t)| \tag{80}$$

It follows that $\bar{\eta}_i(\mathbf{x}_i, \mathbf{x}_r, t) > \eta_i(\mathbf{x}_i, \mathbf{x}_r, \nu_i, t)$ whenever $\delta_i(\mathbf{x}_i, \nu_i, t) > \delta_i^*$. Accordingly, let $\mathcal{D}_i$ be a neighborhood of $(\mathbf{e}_i, \mathbf{e}_r) = (\mathbf{0}_2, \mathbf{0}_2)$, and choose a sliding gain constant η_i^* such that

$$\eta_i^* > \max_{\mathcal{D}_i} \bar{\eta}_i(\mathbf{x}_i, \mathbf{x}_r, t) \tag{81}$$

Then $\dot{V}_i < 0$ holds true along any closed loop trajectory that initiates within $\mathcal{D}_i$ whenever $\delta_i(\mathbf{x}_i, \nu_i, t) \geq \delta_i^*$ and $\eta_i > \eta_i^*$. The existence of a finite number η_i^* is guaranteed for any domain $\mathcal{D}_i$ because $B_i(\mathbf{x}_i, \mathbf{x}_r, t)$ is globally bounded by virtue of implementing the DSGI $\mathcal{A}_i^*$ given by (56) and the nullprojected auxiliary control law $\mathbf{P}_i \boldsymbol{\lambda}_i$ given by (33), which result in globally bounded $\mathbf{e}_i$ and $\mathbf{e}_r$ trajectories, respectively. ■

The following theorem follows.

Theorem 4: Consider the AUV inner subsystem dynamics given by (8) and (10), where $\mathbf{u}_i = \mathbf{u}_i^*$ is the AGDI control law given by (61) and $\boldsymbol{\lambda}_i \in \mathbf{R}^2$ is arbitrary. Then the AUV state dynamics is partially semi-globally practically stable with respect to the equilibrium point $\mathbf{e}_i = \mathbf{0}_{2\times 1}$ of the attitude dynamics given by (8). Moreover, if the auxiliary control law $\mathbf{P}_i(\mathbf{x}_i, t)\boldsymbol{\lambda}_i$ is constructed in the form given by (33) then the AUV state dynamics is partially globally asymptotically stable with respect to the equilibrium point $\mathbf{e}_r = \mathbf{0}_{2\times 1}$ of the angular velocity dynamics given by (10).

Proof: It follows from Theorem 3 that the magnitude of the positive sliding mode gain η_i can always be increased such that an arbitrarily small positive bound δ_i^* is achieved with guaranteeing the condition $\dot{V}_i < 0$ to hold over $\mathcal{D}_i$ whenever $\delta_i(\mathbf{x}_i, \nu_i, t) < \delta_i^*$. Since the attitude error state trajectory $\mathbf{e}_i$ must enter the domain defined by $\delta_i(\mathbf{x}_i, \nu_i, t) < \delta_i^*$ in finite time and remain within that domain, it follows that driving δ_i^* arbitrarily closer to zero implies driving $\mathbf{e}_i$ arbitrarily closer to zero and making it uniformly ultimately bounded, i.e., making $\mathbf{e}_i = \mathbf{0}_{2\times 1}$ practically stable. Moreover, because $\mathcal{D}_i$ can be arbitrarily enlarged by increasing η_i^*, then this practical stability is semi-global. On the other hand, since the auxiliary control law given by (33) is derived via a radially unbounded control Lyapunov function that is positive definite in $\mathbf{e}_r$, then boundedness of $\mathbf{e}_i$ implies global partial asymptotic stability of the AUV dynamics with respect to $\mathbf{e}_r = \mathbf{0}_{2\times 1}$. ■

VII. Simulation Results

To validate the effectiveness of the AGDI autopilot, numerical simulation are carried out in six DOFs simulator of MBARI AUV for the following cases

A. Step profile tracking

In this scenario, the staircase profiles having magnitude of $50m$ and $25m$ are given in the depth and the east directions respectively, assuming nominal marine conditions. The Three Dimensions (3D) position tracking is shown in Fig. 2(a). The actual and the desired attitude profiles are shown in Fig. 2(b). The elevator δ_θ and rudder δ_ψ deflections required to follows attitude commands are shown in Fig. 2(c), whereas the corresponding angular rates are depicted in Fig. 2(d).

B. Helical trajectory tracking

In this plot, the AUV is commanded to follow the helical trajectory in yz_e plane under perturbed environment. Furthermore, 10% variations are also considered in the numerical values of the parameters given by Table I. Initially the AUV is commanded to attain a depth of $30m$ then the sinusoidal trajectories are given in z_e and y_e directions having an amplitude of $10m$ with a phase shift in order to generate the helical trajectory over the range of $10km$.

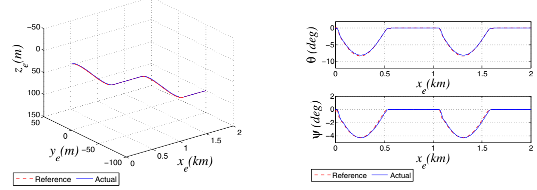

(a) Position tracking

(b) Attitude commands vs. range

(c) Control input vs. range

(d) Body rates vs. range

Fig. 2. Step profile tracking

The positional tracking performance in 3D is shown in Fig. 3(a). The attitude tracking are shown in Fig. 3(b). The control deflections are shown in Fig. 3(c) which is very much realizable, whereas the corresponding body rates are shown in Fig. 3(d).

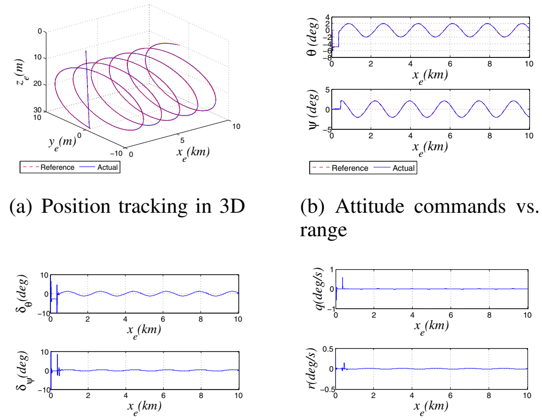

(a) Position tracking in 3D

(b) Attitude commands vs. range

(c) Control input vs. range

(d) Body rates vs. range

Fig. 3. Helical trajectory tracking

VIII. Conclusion

In this paper a two-loops structured control system using AGDI is proposed, in which dynamic constraints are defined successfully in the framework of GDI and its inverse is calculated by incorporating MPGI based Greville formula. The outer position loop successfully generates the desired pitch and yaw attitude commands based on the positional errors. The inner-loop is responsible for the attitude tracking. The null control vector is designed successfully by employing the Lyapunov approach, to stabilize the linear and angular velocities. A dynamic scaling factor is augmented in MPGI to address the singularity problem due to generalized inversion. The integration of SMC with GDI is being performed, to provide robustness and to guarantee semi-global practically stable position and attitude tracking. Numerical simulations are conducted on 6DOF simulator of MBARI AUV, which demonstrate better tracking performance of the AGDI controller and is not influenced by the external disturbances and parametric variations.

References

[1] Y. Xu and K. Xiao, "Technology development of autonomous ocean vehicle," *Acta automatica sinica*, vol. 33, no. 5, p. 518, 2007.

[2] O. Yildiz, A. E. Yilmaz, and B. Gokalp, "State-of-the-art system solutions for unmanned underwater vehicles," *sensors*, vol. 1, p. 2, 2009.

[3] M. Kim, H. Joe, J. Kim, and S.-c. Yu, "Integral sliding mode controller for precise maneuvering of autonomous underwater vehicle in the presence of unknown environmental disturbances," *International Journal of Control*, no. just-accepted, pp. 1–43, 2015.

[4] M. H. Khodayari and S. Balochian, "Modeling and control of autonomous underwater vehicle (auv) in heading and depth attitude via self-adaptive fuzzy pid controller," *Journal of Marine Science and Technology*, vol. 20, no. 3, pp. 559–578, 2015.

[5] I. Eski and S. Yildirim, "Design of neural network control system for controlling trajectory of autonomous underwater vehicles," *International Journal of Advanced Robotic Systems*, vol. 11, 2014.

[6] A. R. Chowdhury, V. Vishwanathan, B. Prasad, R. Kumar, and S. Panda, "Inverse dynamics control of a bio-inspired robotic-fish underwater vehicle propulsion based on lighthill slender body theory," in *OCEANS-TAIPEI*. IEEE, 2014, pp. 1–6.

[7] A. Ben-Israel and T. N. Greville, *Generalized inverses: theory and applications*. Springer Science & Business Media, 2003, vol. 15.

[8] U. Ansari and A. H. Bajodah, "Robust launch vehicles generalized dynamic inversion attitude control," *Aircraft Engineering and Aerospace Technology*, vol. 89, no. 6, pp. 902–910, 2017.

[9] ——, "Robust generalized dynamic inversion based control of autonomous underwater vehicles," *Proceedings of the Institution of Mechanical Engineers, Part M: Journal of Engineering for the Maritime Environment*, p. 1475090217708640, 2017.

[10] ——, "Robust generalized dynamic inversion quadrotor control," *IFAC-PapersOnLine*, vol. 50, no. 1, pp. 8181–8188, 2017.

[11] ——, "Robust generalized inversion control: An application to satellite launch vehicle attitude control," *International Journal of Control Theory and Applications*, vol. 10, no. 34, pp. 93–110, 2017.

[12] ——, "Robust generalized dynamic inversion control of autonomous underwater vehicles," *IFAC-PapersOnLine*, vol. 50, no. 1, pp. 10 658–10 665, 2017.

[13] U. Ansari, A. H. Bajodah, and S. Alam, "Generalized dynamic inversion based attitude control of autonomous underwater vehicles," *IFAC-PapersOnLine*, vol. 49, no. 23, pp. 582–589, 2016.

[14] U. Ansari and A. H. Bajodah, "Guidance and robust generalized inversion based attitude control of satellite launch vehicle," in *4th International Conference on Control Engineering & Information Technology (CEIT)*. IEEE, 2016, pp. 1–6.

[15] ——, "Quadrotor control using generalized dynamic inversion and terminal sliding mode," in *3rd International Conference on Control, Engineering & Information Technology (CEIT)*. IEEE, 2015, pp. 1–6.

[16] ——, "Generalized dynamic inversion scheme for satellite launch vehicle attitude control," *IFAC-PapersOnLine*, vol. 48, no. 9, pp. 114–119, 2015.

[17] R. McEwen and K. Streitlien, "Modeling and control of a variable-length auv," *Proc 12th UUST*, 2001.

[18] I. Hameduddin and A. H. Bajodah, "Nonlinear generalised dynamic inversion for aircraft manoeuvring control," *International Journal of Control*, vol. 85, no. 4, pp. 437–450, 2012.

[19] R. C. Nelson, *Flight stability and automatic control*. WCB/McGraw Hill, 1998, vol. 2.

[20] H. K. Khalil, *Noninear Systems*. Prentice-Hall, New Jersey, 1996.